Electronic supplementary information (ESI)

Boosting charge transfer in Au-decorated B/K co-doped CN nanosheets towards enhanced photocatalytic CO_2 reduction

Xiangli Shi[a], Qiong Zhang[a], Yimeng Zhou[b], Qianjin Ye[b], Deli Jiang[b,*], Dan Tian[c], and Di Li[a,*]

[a] *School of Chemistry and Chemical Engineering, Jiangsu University, 301 Xuefu Road, Zhenjiang 212013, China*

[b] *Institute for Energy Research, Jiangsu University, 301 Xuefu Road, Zhenjiang 212013, China*

[c] *College of Materials Science and Engineering, Nanjing Forestry University, Nanjing 210037, China*

Corresponding authors: Deli Jiang, Di Li

E-mail addresses: dlj@ujs.edu.cn (D. Jiang), cfbgdd@sina.com (D. Li)

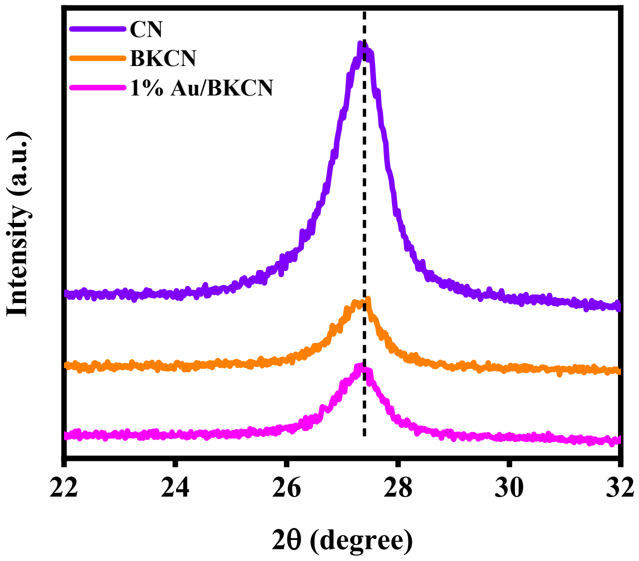

Fig. S1 Enlarged (002) diffraction peak of CN, BKCN and 1% Au/BKCN.

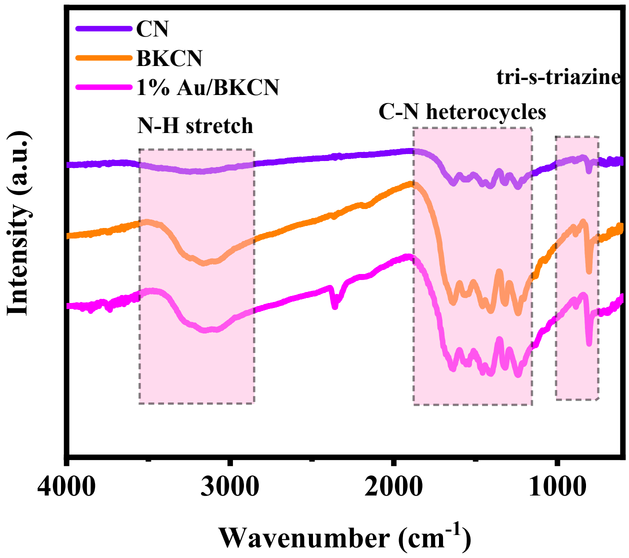

Fig. S2 FTIR spectra of of CN, BKCN and 1% Au/BKCN.

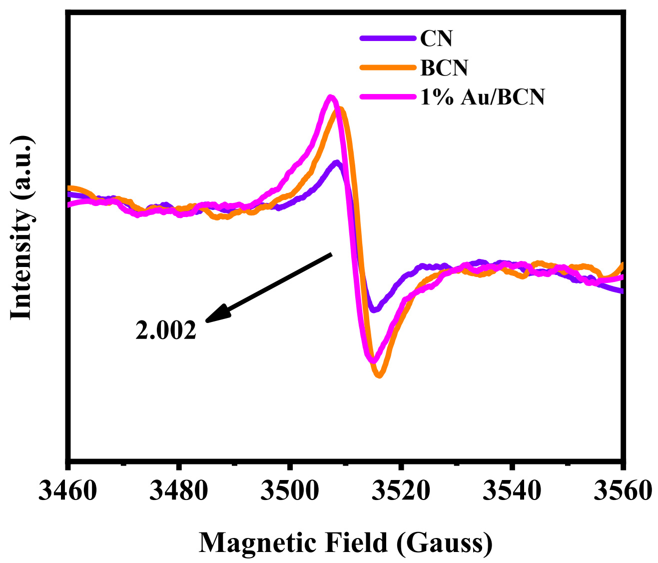

Fig. S3 EPR spectra of CN, BKCN and 1% Au/BKCN.

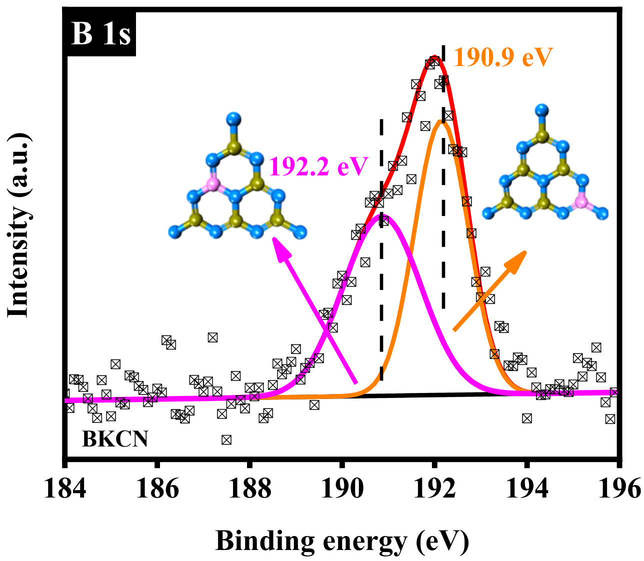

Fig. S4 High-resolution B 1s XPS spectrum of BKCN.

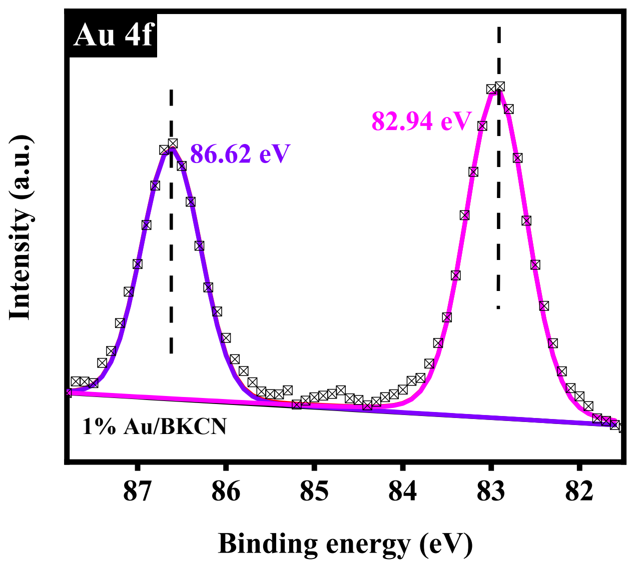

Fig. S5 High-resolution Au 4f XPS spectrum of 1% Au/BKCN.

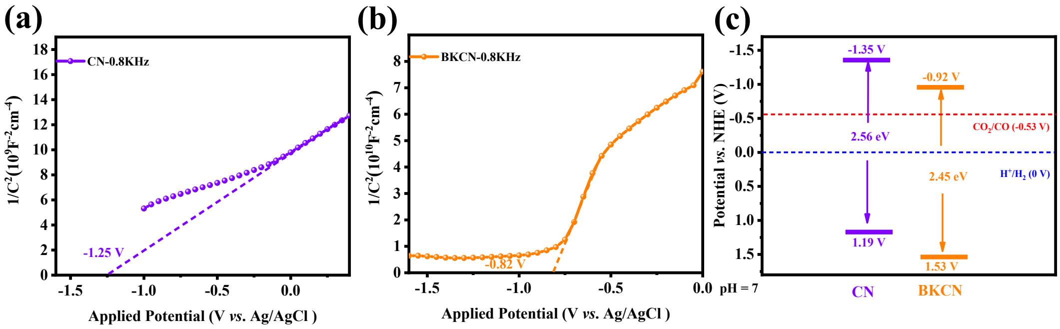

Fig. S6 Mott-Schottky plot of pristine (a) CN and (b) BKCN, and (c) schematic illustration of the band structure of CN and BKCN.

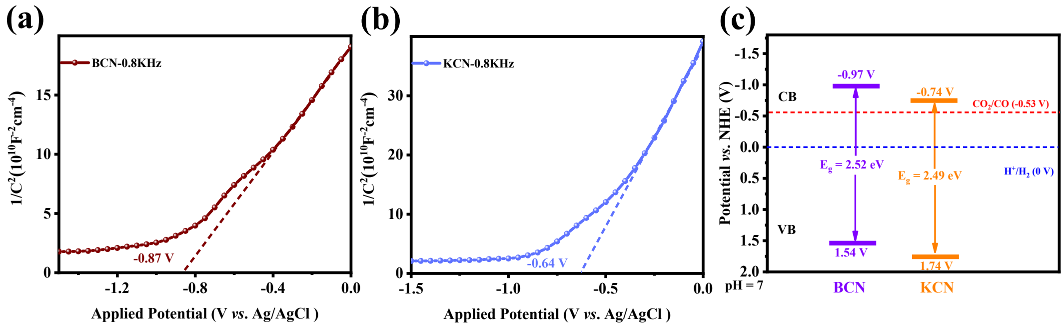

Fig. S7 Mott-Schottky plot of (a) pristine BCN and (b) KCN, and (c) schematic illustration of the band structure of BCN and KCN.

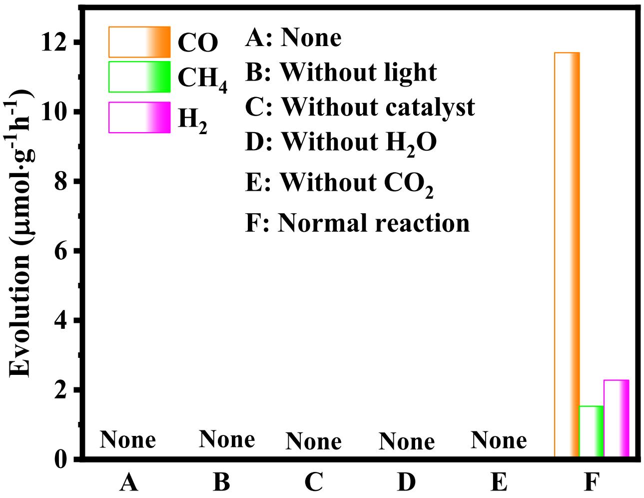

Fig. S8 Photocatalytic CO_2 reduction performance of 1% Au/BKCN under different condition.

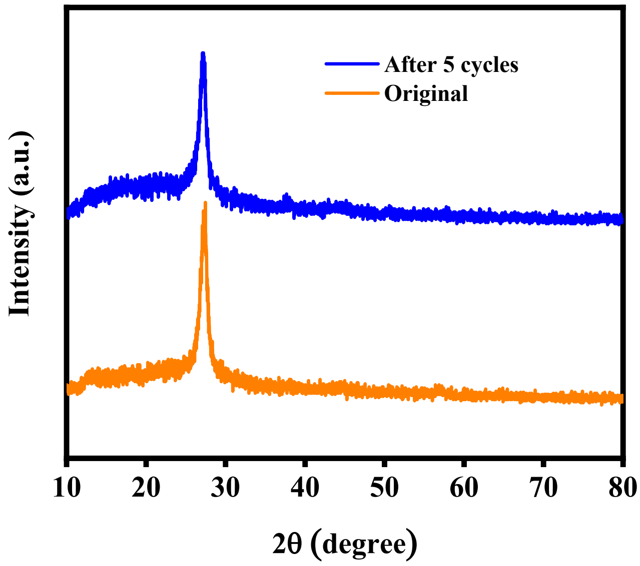

Fig. S9 XRD patterns of 1% Au/BKCN before and after 5 cycles.

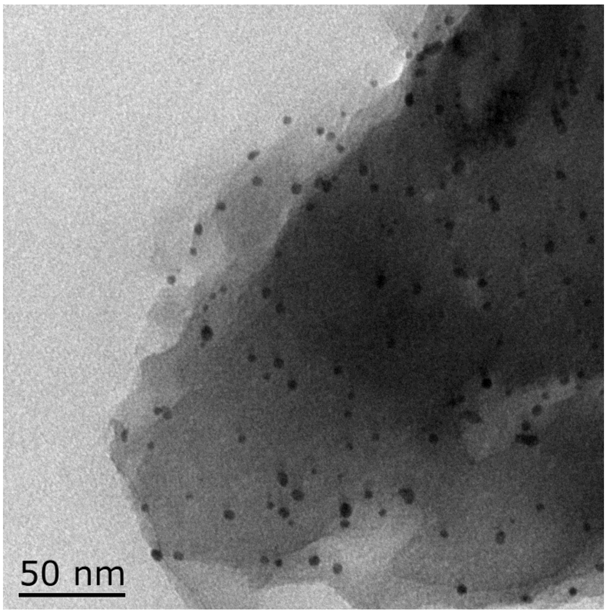

Fig. S10 TEM image of 1% Au/BKCN photocatalyst after five times cycles.

Fig. S11 (a) Products yield of CN, BKCN and 1% Au/BKCN samples through a 500 nm band pass filter. (b) Proposed mechanism for the photocatalytic CO_2 reduction over Au/BKCN under 550 nm monochromatic light.

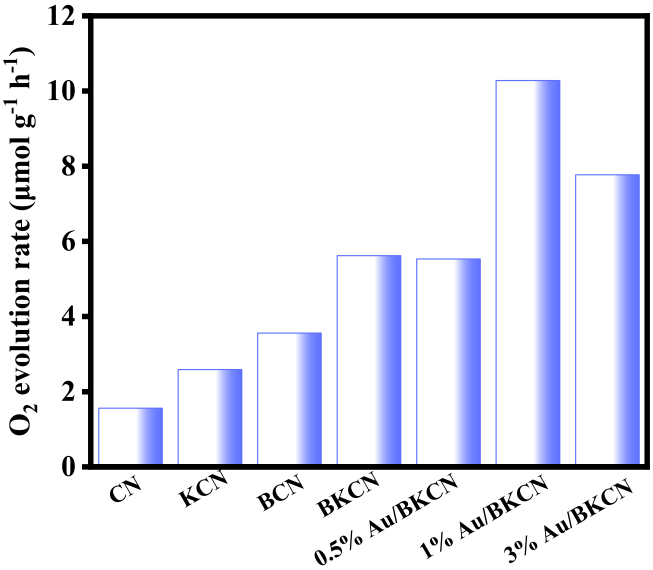

Fig. S12 Yields of O_2 in CO_2 photoreduction.

Table S1. ICP-OES measured Au contents in the as-prepared photocatalysts.

sample	Theoretical Au content (wt.%)	Actual Au content (wt.%)
CN	0	0
BCN	0	0
KCN	0	0
BKCN	0	0
1% Au/CN	1.000	0.960
1% Au/BCN	1.000	1.020
1% Au/KCN	1.000	0.930
0.5% Au/BKCN	0.500	0.550
1% Au/BKCN	1.000	0.980
3% Au/BKCN	3.000	2.970

Table S2. Charge carriers lifetime parameters of CN, BKCN, and 1% Au/BKCN.

Sample	**A_1**	**A_2**	**τ_1 (ns)**	**τ_2 (ns)**	**τ_{ave} (ns)**
CN	36.59	46.77	1.9287	6.0092	5.190
BKCN	39.97	46.78	1.7244	5.7325	4.913
1% Au/BKCN	42.44	43.14	1.7371	5.6751	4.746

Analysis method of time-resolved PL spectra

a "biexponential" function was used to fit the decay curves as follows:

$Fit = A_1e^{(-t/\tau 1)} + A_2e^{(-t/\tau 2)}$

Where the shorter decay lifetime (τ_1) is attributed to the non-radiative relaxation process, and the longer decay lifetime (τ_2) comes from the radiative process which is related to the direct recombination of photoinduced charge carriers. A_1 and A_2 are constants related to non-radiative and radiative relaxation processes, respectively. The average charge carrier lifetime (τ_{ave}) can be calculated from the equation as follows: [$\tau_{ave} = (A_1\tau_1^2 + A_2\tau_2^2)/(A_1\tau_1 + A_2\tau_2)$].

External Quantum Efficiency (EQE) Measurement:

The external quantum efficiency for the photocatalytic CO_2 reduction was determined at 500 nm measured using a single band pass filter by using the same photochemical experimental setup. An area of 38.48 cm^2 was illuminated and the light intensity was measured with a solar power meter (SM206-SOLAR). Light intensity was determined to be 11.6 $W \cdot m^{-2}$. After 5 h irradiation, the CO, CH_4 and H_2 was measured to be 1.6, 0.01, and 0.005 μmol. EQE were calculated using the following equation:

$$EQE(\%) = N_{electron}/N_{photon}$$

The photocatalytic electron consumption ($N_{electron}$) is calculated using the equation:

$$N_{electron} = [2N(CO) + 8N(CH_4) + 2N(H_2)] \times N_A$$

Where, $N(CO)$, $N(CH_4)$, and $N(H_2)$ are the number of moles CO, CH_4, H_2 produced respectively, N_A is Avogadro's number

The photons flux (N_{photon}) is calculated using the equation:

$$N_{photon} = (t \times I \times \lambda \times A)/(h \times c)$$

Where, t is reaction time, I is intensity of light, λ is the wavelength of incident light, and A is the irradiated area, h is Planck constant, c is speed of light. Thus, the external quantum efficiency is estimated to be 0.098%.

Table S3. Comparison of photocatalytic CO_2 reduction based on heteroatoms doped g-C_3N_4.

catalyst	light source	product	reduction yield(μmol g^{-1})	Ref.
Cl-CN	UV (8 W)	CO	39.9	[1]
O-CN	350 W Xe lamp (λ ≥ 420 nm)	C_2H_5OH	4.4	[2]
Au/g-C_3N_4	UV-light (300 W)	CO	16.5	[3]
12FLTC/BCN		CO	14.4	[4]
AUNB/g-C_3N_4	AM 1.5	CO	21.95	[5]
defect g-C_3N_4	UV−vis (300 W Xe lamp)	CO	19.7	[6]
1%Au/BKCN	**300 W Xe lamp**	**CO**	**57.8**	**This work**

References

1 Y. Wang, X. Tang, P. Huo, Y. Yan, Z. Zhu, J. Dai, Z. Liu, Z. Li and H. Xi, Insight into the effect of the Cl 3p orbital on g-C_3N_4 mimicking photosynthesis under CO_2 reduction, *J. Phys. Chem. C*, 2021, **125**, 9646-9656.

2 J. Fu, B. Zhu, C. Jiang, B. Cheng, W. You and J. Yu, Hierarchical porous O-doped g-C_3N_4 with enhanced photocatalytic CO_2 reduction activity, *Small*, 2017, **13**, 1603938.

3 X. Li, C. Liu, D. Wu, J. Li, P. Huo and H. Wang, Improved charge transfer by size-dependent plasmonic Au on C_3N_4 for efficient photocatalytic oxidation of RhB and CO_2 reduction, *Chinese J. Catal.*, 2019, **40**, 928-939.

4 H. Wang, Q. Tang and Z. Wu, Construction of few-layer Ti_3C_2 MXene and boron-doped g-C_3N_4 for enhanced photocatalytic CO_2 reduction, *ACS Sustainable Chem. Eng.*, 2021, **9**, 8425-8434.

5 M. K. Hussien, A. Sabbah, M. Qorbani, M. H. Elsayed, P. Raghunath, T.-Y. Lin, S. Quadir, H.-Y. Wang, H.-L. Wu, D.-L. M. Tzou, M.-C. Lin, P.-W Chung, H.-H. Chou, L.-C. Chen and K.-H. Chen, Metal-free four-in-one modification of g-C_3N_4 for superior photocatalytic CO_2 reduction and H_2 evolution, *Chem. Eng. J.*, 2022, **430**, 132853.

6 W. Ma, N. Wang, Y. Guo, L. Yang, M. Lv, X. Tang and S. Li, Enhanced photoreduction CO_2 activity on g-C_3N_4: by synergistic effect of nitrogen defective-enriched and porous structure, and mechanism insights, *Chem. Eng. J.*, 2020, **388**, 124288.